Geometric phase and topology of elastic oscillations and vibrations in model systems: Harmonic oscillator and superlattice

P. A. Deymier, K. Runge, and J. O. Vasseur

Citation: AIP Advances **6**, 121801 (2016); doi: 10.1063/1.4968608
View online: http://dx.doi.org/10.1063/1.4968608
View Table of Contents: http://scitation.aip.org/content/aip/journal/adva/6/12?ver=pdfcov
Published by the AIP Publishing

Geometric phase and topology of elastic oscillations and vibrations in model systems: Harmonic oscillator and superlattice

P. A. Deymier,[1] K. Runge,[1] and J. O. Vasseur[2]
[1]*Department of Materials Science and Engineering, University of Arizona, Tucson, AZ 85721, USA*
[2]*Institut d'Electronique, de Micro-électronique et de Nanotechnologie, UMR CNRS 8520, Cité Scientifique, 59652 Villeneuve d'Ascq Cedex, France*

(Received 16 August 2016; accepted 24 October 2016; published online 23 November 2016)

We illustrate the concept of geometric phase in the case of two prototypical elastic systems, namely the one-dimensional harmonic oscillator and a one-dimensional binary superlattice. We demonstrate formally the relationship between the variation of the geometric phase in the spectral and wave number domains and the parallel transport of a vector field along paths on curved manifolds possessing helicoidal twists which exhibit non-conventional topology. [http://dx.doi.org/10.1063/1.4968608]

I. INTRODUCTION

From a historical perspective, our scientific understanding of sound and vibrations dates back to Sir Isaac Newton's *Principia*,[1] which examined its first mathematical theory. The mid-19th century book *The Theory of Sound* by Lord Rayleigh[2] still constitutes the foundation of our modern theory of vibrations, whereas the quantum theory of phonons followed in the early part of the 20th century.[3] During this nearly 300-year period, our understanding of sound and elastic waves has been nourished essentially by the paradigm of the plane wave and its periodic counterpart (the Bloch wave) in periodic media. This paradigm relies on the four canonical characteristics of waves: frequency (ω); wave vector ($\boldsymbol{k}$); amplitude ($\boldsymbol{A}$); and phase (φ).

Over the past two decades, the fields of phononic crystals and acoustic metamaterials have developed in which researchers manipulate the spectral and refractive properties of phonons and sound waves through their host material by exploiting ω and $\boldsymbol{k}$.[4] The spectral properties of elastic waves include phenomena such as the formation of stop bands in the transmission spectrum due to Bragg-like scattering or resonant processes, as well as the capacity to achieve narrow band spectral filtering by introducing defects in the material's structure. Negative refraction, zero-angle refraction and other unusual refractive properties utilize the complete characteristics of the dispersion relations of the elastic waves, $\omega(\boldsymbol{k})$, over both frequency and wave number domains.

Recently, renewed attention has been paid to the amplitude and the phase characteristics of the elastic waves. Indeed, it is in the canonical characteristic realms of $\boldsymbol{A}$ and φ where non-conventional new forms of elastic waves reside. This new realm opens gateways to non-conventional forms of elastic wave- or phonon-supporting media. In the most general form of the complex amplitude, $\boldsymbol{A} = A_0 e^{i\varphi}$, elastic oscillations, vibrations and waves can acquire a geometric phase φ which spectral or wave vector dependency can be described in the context of topology. For example, the structure of topological spaces such as manifolds can be used to mirror the properties and constraints imposed on the wave amplitude.

Electronic waves[5] or electromagnetic waves[6–8] with non-conventional topology have been shown to exhibit astonishing properties such as the existence of unidirectional, backscattering-immune edge states. Phononic structures have also been shown recently to possess non-conventional topology as well as topologically constrained propagative properties. These properties have been achieved by

breaking time-reversal symmetry through internal resonance or symmetry breaking structural features (e.g., chirality)[9–19] and without addition of energy from the outside. Energy can also be added to extrinsic topological elastic systems to break time reversal symmetry.[20–26] For example, we have considered the externally-driven periodic spatial modulation of the stiffness of a one-dimensional elastic medium and its directed temporal evolution to break symmetry.[26] The bulk elastic states of this time-dependent super-lattice possess non-conventional topological characteristics leading to non-reciprocity in the direction of propagation of the waves.

Topological elastic oscillations, vibrations and waves promise designs and new device functionalities which require a deeper insight into the relationship between geometric phase and topology. It is the objective of this paper to shed light on this relation. In particular, in the present paper, we employ two prototypical elastic model systems, namely the one-dimensional harmonic oscillator and a one-dimensional elastic binary superlattice to demonstrate analytically and formally the relationship between the variation of the geometric phase in the spectral and wave number domains and its topological interpretation in terms of the parallel transport of a vector field along paths in frequency or wave vector on a curved manifold, namely strips containing a local helicoidal twist.

In section 2, we introduce the formalism to describe the geometric phase of the amplitude of a one-dimensional harmonic oscillator in its spectral domain. A detailed topological interpretation of this phase in a curved space is also derived. In section 3, we consider a one-dimensional binary superlattice and its dispersion characteristics. We analyze the amplitude of elastic wave supported by this superlattice in the wave number domains and pay particular attention to elastic bands that accumulate a non-zero geometric phase within the Brillouin zone. The topological interpretation of the evolution of the phase along a path in wave number space (i.e. Brillouin zone) is formally established. Finally, we draw a series of conclusions in section 4 which provide a foundation for the formal topological description of elastic waves in more complex phononic crystals and acoustic metamaterials structures.

II. HARMONIC OSCILLATOR MODEL SYSTEMS

In this section, we consider, two model systems, namely a simple one-dimensional harmonic oscillator and the driven harmonic oscillator. In both cases we illustrate the concept of geometric phase and develop the formalism necessary to interpret it in the context of topology.

A. Geometric phase and dynamical phase of the damped harmonic oscillator

The dynamics of the damped harmonic oscillator is given by:

$$\frac{\partial^2 \tilde{u}(t)}{\partial t^2} + \mu \frac{\partial \tilde{u}(t)}{\partial t} + \omega_0^2 \tilde{u}(t) = 0. \tag{1}$$

Here, μ is the damping coefficient and ω_0 is the characteristic frequency. $\tilde{u}(t)$ is the displacement of the oscillator. We rewrite this equation in the form:

$$\frac{\partial^2 u(\xi,t)}{\partial t^2} + \mu \frac{\partial u(\xi,t)}{\partial t} = -i \frac{\partial u(\xi,t)}{\partial \xi}. \tag{2}$$

To obtain equation (2), we have defined: $u(\xi,t) = \tilde{u}(t) e^{-i\omega_0^2 \xi}$. We generalize Eq. (2) further by introducing the equation:

$$\frac{\partial^2 u(\xi,t)}{\partial t^2} - i\varepsilon\phi(\xi) \frac{\partial u(\xi,t)}{\partial t} = -i \frac{\partial u(\xi,t)}{\partial \xi}. \tag{3}$$

The damped oscillator is recovered when $i\varepsilon\phi(\xi) = -\mu$. Here ε and ϕ are a parameter and a function, respectively. In the limit of small ε (i.e. to first order), we can perform the following substitution:

$$\frac{\partial^2 u(\xi,t)}{\partial t^2} - i\varepsilon\phi(\xi) \frac{\partial u(\xi,t)}{\partial t} \sim \left(\frac{\partial}{\partial t} - i\varepsilon \frac{\phi(\xi)}{2} \right)^2 u(\xi,t). \tag{4}$$

With this substitution, equation (3) takes the form of the one-dimensional Schroedinger equation in the presence of a magnetic field:

$$-i\frac{\partial u(\xi,t)}{\partial \xi} = \left(\frac{\partial}{\partial t} - i\varepsilon\frac{\phi(\xi)}{2}\right)^2 u(\xi,t), \tag{5}$$

where ξ plays the role of time and t plays the role of position. ϕ acts as a single component vector potential associated with the magnetic field. The term in parenthesis plays the role of the canonical momentum of a charged particle in a magnetic field. If we choose a solution of the form:

$$u(\xi,t) = v(\omega(\xi),t)e^{-i\omega_0^2\xi} \quad \text{with} \quad v(\omega(\xi),t) = \tilde{v}(\omega(\xi))e^{i\omega(\xi)t}, \tag{6}$$

and insert it into equation (5), we obtain:

$$\omega_0^2 = \left[\omega(\xi) - \varepsilon\frac{\phi(\xi)}{2}\right]^2. \tag{7}$$

Equation (7) states that $\omega(\xi) = \omega_0 + \varepsilon\frac{\phi(\xi)}{2}$. The function $\phi(\xi)$ offers a mechanism for tuning/driving the frequency of the oscillator around its characteristic frequency.

We now assume that the solution to equation (5) may carry a phase $\eta(\omega(\xi))$ that depends on the frequency. This solution is therefore rewritten in the form:

$$u_\eta(\xi,t) = u(\xi,t)e^{i\eta(\omega(\xi))} = v(\omega(\xi),t)e^{-i\omega_0^2\xi}e^{i\eta(\omega(\xi))}. \tag{8}$$

Inserting this solution into Eq. (5) yields:

$$i\left(\frac{\partial u}{\partial \xi}e^{i\eta} + u_\eta i\frac{\partial \eta}{\partial \omega}\frac{\partial \omega}{\partial \xi}\right) = \left[\omega(\xi) - \varepsilon\frac{\phi(\xi)}{2}\right]^2 u_\eta. \tag{9}$$

We multiply both sides of this equation by the complex conjugate: $u_\eta^* = u^* e^{-i\eta}$. After some manipulations we get:

$$\frac{\partial \eta}{\partial \omega} = iu^*\frac{\partial u}{\partial \xi}\frac{\partial \xi}{\partial \omega} - \left[\omega(\xi) - \varepsilon\frac{\phi(\xi)}{2}\right]^2\frac{\partial \xi}{\partial \omega}.$$

This equation reveals the change in phase of the oscillator:

$$d\eta = iu^*\frac{\partial u}{\partial \omega}d\omega - \left[\omega(\xi) - \varepsilon\frac{\phi(\xi)}{2}\right]^2 d\xi. \tag{10}$$

The first term on the right hand side of Eq. (10) contains the Berry connection defined as $-iu^*\frac{\partial u}{\partial \omega}$.[27] Indeed, since $u(\xi,t) = \tilde{u}(t)e^{-i\omega_0^2\xi}$, then $iu^*\frac{\partial u}{\partial \omega} = i\tilde{u}^*\frac{\partial \tilde{u}}{\partial \omega}$ where $\tilde{u}$ is the solution of Eq. (1). Equation (10) can be integrated along a path in eigen value space driven by the parameter ξ.

$$\int_{\xi_1}^{\xi_2} d\eta = \int_{\omega(\xi_1)}^{\omega(\xi_2)} i\tilde{u}^*\frac{\partial \tilde{u}}{\partial \omega}d\omega - \int_{\xi_1}^{\xi_2}\left[\omega(\xi) - \varepsilon\frac{\phi(\xi)}{2}\right]^2 d\xi. \tag{11}$$

The second term on the right-hand side of Eq. (11) is the dynamical phase. The first term on the right-hand side of Eq. (11) is the geometrical phase. Here we have used the parameter ξ to vary the frequency of the oscillator. In the next subsection, we will use a driving force to achieve the same result, i.e., we will consider the case of the driven harmonic oscillator. Both approaches provide a similar description of the evolution of the phase of the propagating waves in the space of the eigen values of the system.

B. Geometrical phase of the driven harmonic oscillator

The dynamics of the driven harmonic oscillator is given by:

$$\frac{\partial^2 u}{\partial t^2} + \omega_0^2 u = ae^{i\omega t}, \tag{12}$$

where u is the displacement. ω_0 is again the characteristic frequency of the oscillator. ω is the angular frequency of the driving function and the parameter a has the dimension of an acceleration. To solve this equation, we seek solutions of the form:

$$u(t) = u_0(\omega)e^{i\omega t}. \tag{13}$$

Inserting Eq. (13) into Eq. (12), leads to:

$$\left(-\omega^2 + \omega_o^2\right) u_0 = a. \tag{14}$$

We note that Eq. (12) is the spectral decomposition of the following equation:

$$\left(\frac{\partial^2}{\partial t^2} + \omega_0^2\right) U = a.\delta(t), \tag{15}$$

with $\delta(t) = \int_{-\infty}^{+\infty} e^{i\omega t} d\omega$ and $U(t) = \int_{-\infty}^{+\infty} u_0(\omega)e^{i\omega t} d\omega$. U in Eq. (15) is a Green's function if $a = 1$ $m.s^{-2}$. $u_0(\omega)$ is then its spectral representation.

From equation (14), we get:

$$u_0\left(\omega^2\right) = \frac{1}{\left(\omega_o^2 - \omega^2\right)} \sim \frac{1}{\left(\omega_o^2 - \omega^2 - i\varepsilon\right)} = \frac{1\left(\omega_o^2 - \omega^2 + i\varepsilon\right)}{\left(\omega_o^2 - \omega^2\right)^2 + \varepsilon^2}. \tag{16}$$

In Eq. (16) we have analytically continued the solution into the complex plane by introducing an imaginary term $-i\varepsilon$ with $\varepsilon \to 0$. It is important to keep in mind that the eigen values are now denoted $E = \omega^2$. To calculate the Berry connection, $BC(E)$, we use the first term on the right hand side of Eq. (10) where ω^2 is replaced by E:

$$BC(E) = -i\hat{u}_0^*(E)\frac{d\hat{u}_0(E)}{dE} = \frac{-\varepsilon}{\left(\omega_o^2 - \omega^2\right)^2 + \varepsilon^2}. \tag{17}$$

$\hat{u}_0$ in Eq. (17) is the normalized Green's function.

It is interesting to take the limit of Eq. (17) when $\varepsilon \to 0$. For this we can use the well-known identity: $\lim_{\varepsilon \to 0} \frac{\varepsilon}{x^2 + \varepsilon^2} = \pi\delta(x)$. In that limit, the Berry connection becomes:

$$BC(E) = -\pi\delta\left(\omega_0^2 - E\right). \tag{18}$$

This expression can be reformulated in terms of frequencies by using the identity: $\delta\left(x^2 - b^2\right) = \frac{1}{2b}\left(\delta(x - b) + \delta(x + b)\right)$ for $b > 0$. In the positive frequency range, the Berry connection becomes:

$$BC(E) = -\pi\frac{1}{2\omega_0}\delta(\omega - \omega_0). \tag{19}$$

Now using Eq. (10), we can determine the phase change from the relation:

$$BC(E) = \frac{d\eta(E)}{dE} = \frac{d\eta(\omega)}{2\omega d\omega} = -\pi\frac{1}{2\omega_0}\delta(\omega - \omega_0), \tag{20}$$

so we obtain

$$\frac{d\eta(\omega)}{d\omega} = -\pi\frac{\omega}{\omega_0}\delta(\omega - \omega_0). \tag{21}$$

The variation in phase of the displacement amplitude, u_0, over some range of frequency: $[\omega_1, \omega_2]$ is now obtained by integration (see Eq. (11)):

$$\Delta\eta_{1,2} = -\pi\int_{\omega_1}^{\omega_2} d\omega\frac{\omega}{\omega_0}\delta(\omega - \omega_0). \tag{22}$$

There is no phase change for intervals with both frequencies below the characteristic frequency and for intervals with both frequencies above the characteristic frequency, as well. However, by tuning the driving frequency from below the characteristic frequency to above, ω_0, the amplitude of the oscillation accumulates a -π phase difference. The oscillator changes from being

in phase to being out of phase with the driving force. This means that the amplitude of the oscillation changes sign at the characteristic frequency (this is clear from Eq. (16) in the limit of $\varepsilon \to 0$).

C. Topological interpretation of the geometrical phase

In this subsection, we construct a manifold whose topology leads to the same geometrical phase characteristics as the driven harmonic oscillator i.e., Eq. (21). We consider first a three-dimensional helicoid manifold (see figure 1) which parametric equation is given by:

$$\vec{r}(r,\phi) = X(r,\phi)\vec{i} + Y(r,\phi)\vec{j} + Z(r,\phi)\vec{k} = r\cos\phi\vec{i} + r\sin\phi\vec{j} + c\phi\vec{k}. \tag{23}$$

The parameter c is the pitch of the helicoid.

An element of length on the manifold is:

$$\begin{aligned} d\vec{s} &= dX\vec{i} + dY\vec{j} + dZ\vec{k} = dr\left(\cos\phi\vec{i} + \sin\phi\vec{j}\right) + d\phi\left(-r\sin\phi\vec{i} + r\cos\phi\vec{j} + c\vec{k}\right), \\ &= dr\vec{e}_r + d\phi\vec{e}_\phi \end{aligned} \tag{24}$$

where the vectors $\vec{e}_r$ and $\vec{e}_\phi$ are the tangent vectors of the helicoid. We normalize these tangent vectors, and we introduce the vector $\vec{e}_n = \vec{e}_r \times \vec{e}_\phi$ to form the helicoidal coordinate system:

$$\vec{e}_r = \cos\phi\vec{i} + \sin\phi\vec{j}, \tag{25a}$$

$$\vec{e}_\phi = \frac{1}{\sqrt{r^2 + c^2}}\left(-r\sin\phi\vec{i} + r\cos\phi\vec{j} + c\vec{k}\right), \tag{25b}$$

$$\vec{e}_n = \frac{1}{\sqrt{r^2 + c^2}}\left(c\sin\phi\vec{i} - c\cos\phi\vec{j} + r\vec{k}\right). \tag{25c}$$

The affine connection is defined through the derivative in the manifold of the coordinate basis vector projected onto the tangent vectors, namely:[28]

$$\frac{\partial\vec{e}_\alpha}{\partial\beta} = \Gamma^\gamma_{\alpha\beta}\vec{e}_\gamma, \tag{26}$$

where $\alpha, \beta, \gamma = r, \phi$. In Eq. (26), we have used the Einstein notation where summation on the repeating indices (here γ) is implicit.

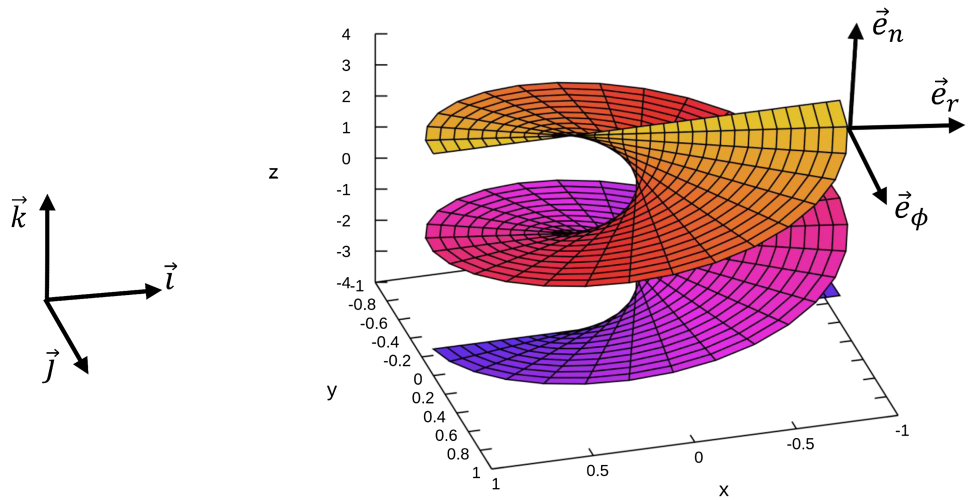

FIG. 1. Schematic representation of a helicoid. $(\vec{i},\vec{j},\vec{k})$ is a fixed Cartesian coordinate system and $(\vec{e}_r, \vec{e}_\phi, \vec{e}_n)$ is the local coordinate system.

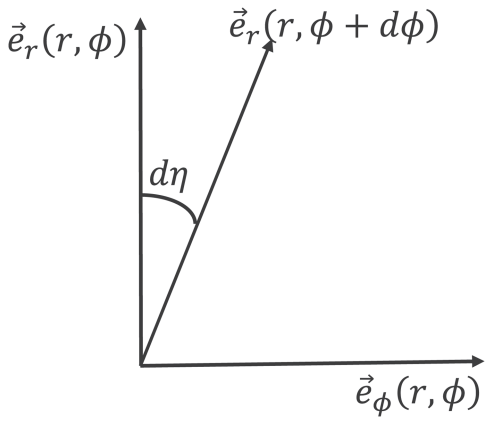

FIG. 2. Schematic illustration of the connection $d\eta \cong \Gamma^{\phi}_{\phi r}$ in the system of coordinate $(\vec{e}_r, \vec{e}_\phi, \vec{e}_n)$.

We now calculate the connection component, $\Gamma^{\phi}_{\phi r}$:

$$\Gamma^{\phi}_{\phi r} = \vec{e}_\phi(r,\phi).\vec{e}_r(r,\phi+d\phi) \cong \vec{e}_\phi(r,\phi).\vec{e}_r(r,\phi) + \vec{e}_\phi(r,\phi)\frac{\partial \vec{e}_r(r,\phi)}{\partial\phi}d\phi + \ldots \tag{27}$$

The first term on the right hand side of Eq. (27) is zero by virtue of the orthogonality of the coordinate system. The derivative in the second term can be determined in the fixed Cartesian coordinate system $(\vec{i},\vec{j},\vec{k})$ and converted in the $(\vec{e}_r, \vec{e}_\phi, \vec{e}_n)$ coordinate system:

$$\frac{\partial \vec{e}_r(r,\phi)}{\partial\phi} = \frac{r}{\sqrt{r^2+c^2}}\vec{e}_\phi(r,\phi) - \frac{c}{\sqrt{r^2+c^2}}\vec{e}_n. \tag{28}$$

This leads to the connection:

$$\Gamma^{\phi}_{\phi r} \cong \vec{e}_\phi(r,\phi)\frac{\partial \vec{e}_r(r,\phi)}{\partial\phi}d\phi = \frac{r}{\sqrt{r^2+c^2}}d\phi. \tag{29}$$

As illustrated in Fig. 2, we note that $\vec{e}_\phi(r,\phi).\vec{e}_r(r,\phi+d\phi) = \sin(d\eta) \cong d\eta$. Here $d\eta$ is the change in angle of the vector $\vec{e}_r$ as one varies the parameter ϕ.

Therefore, we can write:

$$d\eta \cong \Gamma^{\phi}_{\phi r} \cong \frac{r}{\sqrt{r^2+c^2}}d\phi, \quad \text{or} \quad \frac{d\eta}{d\phi} \cong \frac{r}{\sqrt{r^2+c^2}}. \tag{30}$$

We now construct the manifold of interest out of a helicoid with pitch $c = 2\Delta\omega$ by introducing a parametrization in terms of the frequency, ω: $\phi(\omega) = \frac{\pi}{\Delta\omega}\left(\omega - \left(\omega_0 - \frac{\Delta\omega}{2}\right)\right)$ for $\omega_0 - \frac{\Delta\omega}{2} \le \omega \le \omega_0 + \frac{\Delta\omega}{2}$ and $\phi(\omega)$ is a constant otherwise. The limit of this function when $c = \Delta\omega \to 0$ is the Heaviside function whose derivative is the Dirac delta function. This construction leads to the manifold illustrated in Fig. 3.

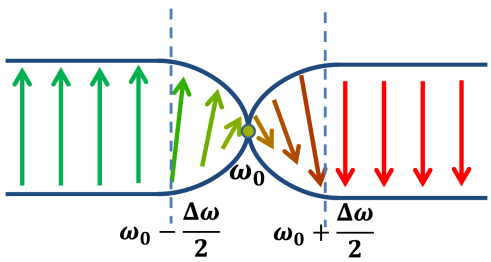

FIG. 3. Schematic illustration of a manifold with a single half-turn twist, its topology is isomorphic to that of the eigen vectors of the harmonic oscillator near resonance.

This manifold may be visualized as a strip with one single half-turn twist. The segment of helicoid represents the twisted region. In the limit $c = \Delta\omega \to 0$ the twisted region becomes infinitesimally narrow.

With this parametrization, the angle η changes according to: $\frac{d\eta}{d\omega} \cong \frac{r}{\sqrt{r^2+c^2}}\frac{d\phi}{d\omega} = \frac{r}{\sqrt{r^2+c^2}}\frac{\pi}{\Delta\omega}$ for $\omega_0 - \frac{\Delta\omega}{2} \le \omega \le \omega_0 + \frac{\Delta\omega}{2}$ and $\frac{d\eta}{d\omega} = 0$ otherwise. In the limit $c = \Delta\omega \to 0$, the angle variation becomes:

$$\frac{d\eta}{d\omega} \cong \pi\delta(\omega - \omega_0). \tag{31}$$

To within an unimportant sign, this equation is isomorphic to equation (21) that described the change in phase of a harmonic oscillator through resonance along the space of its eigen values. The topology of the eigen vectors of the harmonic oscillator is therefore isomorphic to that of a manifold constituted of a twisted strip with an infinitesimally narrow twist.

The topology of a system with multiple resonances may be visualized by a manifold with a sequence of twists along the frequency axis. The properties of the phase of the displacement of the harmonic oscillator can be visualized by the parallel transport of a vector field parallel to the twisted strip manifold. This point is illustrated below. Let consider some parametric curve, **C**, on the helicoid manifold, $x^\alpha(\omega) = (r(\omega), \phi(\omega))$ with $\alpha = r, \phi$. The parameter ω enables us to move along the curve. Let us also consider some vector field $\vec{v}(\omega) = v^\alpha(\omega)\vec{e}_\alpha(\omega)$ at any point along the curve **C**. Here $\vec{e}_\alpha(\omega)$ correspond to the coordinate basis vectors at a point on the curve. The derivative of the vector, $\vec{v}$, along the curve if given by:

$$\frac{d\vec{v}}{d\omega} = \frac{dv^\alpha}{d\omega}\vec{e}_\alpha + v^\alpha\frac{d\vec{e}_\alpha}{d\omega} = \frac{dv^\alpha}{d\omega}\vec{e}_\alpha + v^\alpha\frac{\partial\vec{e}_\alpha}{\partial x^\beta}\frac{dx^\beta}{d\omega}. \tag{32}$$

Substituting for $\frac{\partial\vec{e}_\alpha}{\partial x^\beta}$ using Eq. (26), we can write Eq. (32) in terms of the connection:

$$\frac{d\vec{v}}{d\omega} = \frac{dv^\alpha}{d\omega}\vec{e}_\alpha + v^\alpha\Gamma^\gamma_{\alpha\beta}\vec{e}_\gamma\frac{dx^\beta}{d\omega}.$$

The dummy indices α and γ can be interchanged such that we can factor out the basis vectors:

$$\frac{d\vec{v}}{d\omega} = \left(\frac{dv^\alpha}{d\omega} + v^\gamma\Gamma^\alpha_{\gamma\beta}\frac{dx^\beta}{d\omega}\right)\vec{e}_\alpha. \tag{33}$$

The term in parentheses is defined as the absolute derivative

$$\frac{Dv^\alpha}{D\omega} = \frac{dv^\alpha}{d\omega} + v^\gamma\Gamma^\alpha_{\gamma\beta}\frac{dx^\beta}{d\omega}. \tag{34}$$

Let us suppose that the condition: $\frac{d\vec{v}}{d\omega} = 0$ is always satisfied along the curve **C**. This condition defines the notion of parallelism of the vector field $\vec{v}$ as the vector is transported along the curve. In the case of the manifold of Fig. 3 with a segment of helicoid connected to two flat strips, if we choose $\vec{v} = v^r\vec{e}_r$ (i.e.$v^r = 1$ and $v^\phi = 0$) then we can show that $\frac{Dv^r}{D\omega} = 0 + \Gamma^r_{r\phi}\frac{dx^\phi}{d\omega} + \Gamma^r_{rr}\frac{dx^r}{d\omega}$. The last term in this expression $\frac{dx^r}{d\omega} = \frac{dr}{d\omega}$ is zero because r is independent of ω. We also have $\frac{dx^\phi}{d\omega} = \frac{d\phi}{d\omega} \neq 0$ for $\omega_0 - \frac{\Delta\omega}{2} \le \omega \le \omega_0 + \frac{\Delta\omega}{2}$ and from Eq. (26): $\Gamma^r_{r\phi} = 0$. By consequence, $\frac{d\vec{e}_r}{d\omega} = 0$ for $\omega_0 - \frac{\Delta\omega}{2} \le \omega \le \omega_0 + \frac{\Delta\omega}{2}$, that is $\vec{e}_r$ satisfies the condition for parallel transport along the segment of helicoid in Fig. 3. Outside the interval: $\omega_0 - \frac{\Delta\omega}{2} \le \omega \le \omega_0 + \frac{\Delta\omega}{2}$, $\frac{d\phi}{d\omega} = 0$, $\frac{d\vec{e}_r}{d\omega} = 0$ because the manifold is a planar strip. The parallel transported vector is illustrated in Fig. 3 as colored arrows.

The structure of the manifold in the eigen value space, ω, composed of a strip subjected to a local helicoidal twist mirrors the properties and constraints imposed on the oscillation amplitude. In particular parallel transport on that manifold shows a rotation of π of the vector field at resonance. From an experimental point of view, the amplitude of driven oscillations change sign across the resonance, that is the oscillations are in phase with the forcing function below resonance and out of phase with the forcing function for frequencies above resonance.

III. ELASTIC SUPERLATTICE MODEL SYSTEM

A. Geometrical phase of a one-dimensional elastic superlattice: Zak phase

The geometric phase that characterizes the property of bulk bands in one-dimensional (1D) periodic systems is also known as the Zak phase.[29] In this section, we illustrate the concept of Zak phase in the case of a 1D elastic superlattice.[30,31] We consider a 1D elastic superlattice constituted of layers composed of alternating segments of material 1 and material 2 (Fig. 4) with density and speed of sound ρ_1, ρ_2 and c_1, c_2. The lengths of the alternating segments are d_1 and d_2, respectively. The period of the superlattice is $L = d_1 + d_2$.

In the appendix, we find solutions for the displacement inside segment 1 in layer n in the form:

$$u_1(x,t) = e^{iqnL}\left(A_+ e^{ik_1(x-nL)} + A_- e^{-ik_1(x-nL)}\right)e^{i\omega t}, \tag{35}$$

with the amplitudes

$$A_+ = \frac{1}{2}\left(F - \frac{1}{F}\right)\sin k_1 d_1 \sin k_2 d_2 + \frac{i}{2}\left(F - \frac{1}{F}\right)\cos k_1 d_1 \sin k_2 d_2, \tag{36a}$$

$$A_- = i\left[\sin k_1 d_1 \cos k_2 d_2 + \frac{1}{2}\left(F + \frac{1}{F}\right)\cos k_1 d_1 \sin k_2 d_2 - \sin qL\right], \tag{36b}$$

and the dispersion relation, $\omega(q)$, given by the relation:

$$\cos qL = \cos k_1 d_1 \cos k_2 d_2 - \frac{1}{2}\left(F + \frac{1}{F}\right)\sin k_1 d_1 \sin k_2 d_2. \tag{37}$$

In these equations, $F = \frac{k_1\rho_1 c_1^2}{k_1\rho_1 c_1^2}$ with $k_1 = \frac{\omega}{c_1}$ and $k_2 = \frac{\omega}{c_2}$. The wave number $q \in \left[\frac{-\pi}{L}, \frac{\pi}{L}\right]$.

From Eq. (36a), one observes that when $\sin k_2 d_2 = 0$, the amplitude $A_+ = 0$. Let us consider an isolated band in the band structure of the superlattice for which this condition is satisfied. Under this condition the dispersion relation simplifies to:

$$\cos qL = \cos(k_1 d_1 + k_2 d_2). \tag{38}$$

To obtain Eq. (38), we used the trigonometric relation:

$$\cos k_1 d_1 \cos k_2 d_2 - \sin k_1 d_1 \sin k_2 d_2 = \cos(k_1 d_1 + k_2 d_2).$$

Under this same condition the amplitude A_- reduces to:

$$A_- = i\left[\sin k_1 d_1 \cos k_2 d_2 - \sin qL\right],$$

or using standard trigonometric relations

$$A_- = i\left[\sin(k_1 d_1 + k_2 d_2) - \sin qL\right]. \tag{39}$$

When the wave number is in the positive half of the Brillouin zone i.e. $qL \in [0, \pi]$, Eq. (38) is satisfied when $k_1 d_1 + k_2 d_2 = qL + m2\pi$ with m being an integer. In this case, $\sin(k_1 d_1 + k_2 d_2) - \sin qL = 0$, that is $A_- = 0$. Therefore, we conclude that when $\sin k_2 d_2 = 0$ and $q>0$ both amplitudes A_+ and A_- becomes zero (so does the displacement field).

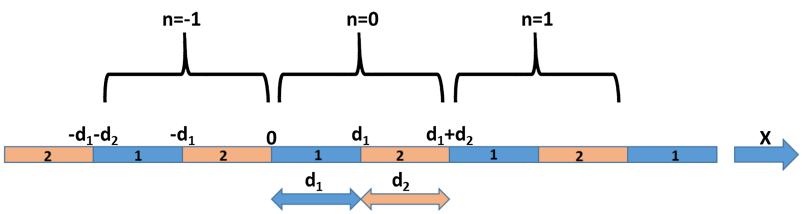

FIG. 4. Schematic representation of the one-dimensional superlattice. A layer, n, is composed of two adjacent segments. The period of the super lattice is $L = d_1 + d_2$.

When the wave number is negative, i.e. $qL \in [-\pi, 0]$, Eq. (38) is satisfied when $k_1 d_1 + k_2 d_2 = |q| L + 2m\pi$ (note that $k_1 d_1 + k_2 d_2 > 0$). In this case, $\sin(k_1 d_1 + k_2 d_2) = \sin(|q| L + 2m\pi) = \sin |q| L$ and $\sin(k_1 d_1 + k_2 d_2) - \sin qL \neq 0$, the amplitude $A_- \neq 0$ and the displacement field does not vanish.

Let us define the point along the dispersion curve where the displacement amplitudes vanish by (q_0, ω_0). We have at this point $k_2 d_2 = \frac{\omega_0(q_0)}{c_2} d_2 = m\pi$ where m is an integer. We now calculate the slope of A_+ and A_- as functions of q. Using Eqs. (36a,b) and the dispersion relation (37) as well as its derivative, we obtain after numerous steps:

$$\frac{dA_+}{dq} = \frac{1}{2}\left(F + \frac{1}{F}\right)\left\{d_1 \frac{dk_1}{dq}\left(\cos k_1 d_1 - i \sin k_1 d_1\right) \sin k_2 d_2 + d_2 \frac{dk_2}{dq}\left(\sin k_1 d_1 + i \cos k_1 d_1\right) \cos k_2 d_2\right\},$$

and

$$\frac{dA_-}{dq} = L \cos qL \left\{\frac{\sin qL - \frac{1}{L}\cos k_1 d_1 \sin k_2 d_2 \left(d_2 \frac{dk_2}{dq} + \frac{1}{2}\left(F + \frac{1}{F}\right) d_1 \frac{dk_1}{dq}\right)}{\sin k_1 d_1 \cos k_2 d_2} - 1\right\}.$$

At the point (q_0, ω_0), $\sin k_2 d_2 = 0$ and $\sin k_1 d_1 \cos k_2 d_2 = \sin(k_1 d_1 + k_2 d_2)$ and

$$\left.\frac{dA_+}{dq}\right|_{q_0} = \frac{1}{2}\left(F + \frac{1}{F}\right)\left\{\frac{dk_2}{dq}\left(\sin k_1 d_1 + i \cos k_1 d_1\right)(-1)^m\right\},$$

and

$$\left.\frac{dA_-}{dq}\right|_{q_0} = L \cos qL \left\{\frac{\sin qL}{\sin(k_1 d_1 + k_2 d_2)} - 1\right\}.$$

We have $\left.\frac{dA_+}{dq}\right|_{q_0} \neq 0$ and $\left.\frac{dA_-}{dq}\right|_{q_0} = 0$ on one side of the Brillouin zone (at q_0) where $\sin(k_1 d_1 + k_2 d_2) = \sin qL$. Therefore, when following a path along the dispersion curve, the amplitude A_+ changes sign when crossing (q_0, ω_0) and therefore its phase changes by π. Along the same path, the amplitude A_- does not change sign.

In Fig. 5, we illustrate the concept of Zak phase for a particular case. We have chosen the following parameters: $\frac{d_2}{c_2} = 1.2\frac{d_1}{c_1}$ and $F = 2$. The band structure of the superlattice is shown in Fig. 5(a) with its usual band folding and formation of band gaps at the origin and the edges of the Brillouin zone. The band structure is obtained by solving for qL for various values of reduced frequency $\omega \frac{d_1}{c_1}$ using Eq. (37). In Figs. 5(b) and 5(c), we have plotted the real part and imaginary part of A_+ and the imaginary part of A_- for two isolated dispersion branches, namely the second and third branches. One notices that the amplitude A_+ as functions of $qL \in [-\pi, \pi]$ cross and change sign in the case of the second branch, at $q_0 L = 0.524$. The amplitude A_- reaches zero there but does not change sign (its slope is zero). The amplitudes do not cross at a value of 0 in Fig. 5(c). This behavior repeats for the 4th, 5th etc. bands.

The amplitudes A_+ and A_- are now expanded in a series around the point q_0:

$$A_+(q) = A_+(q_0) + \left.\frac{dA_+}{dq}\right|_{q_0}(q - q_0) + \ldots \approx \left.\frac{dA_+}{dq}\right|_{q_0} \delta q, \tag{40}$$

and

$$A_-(q) = A_-(q_0) + \left.\frac{dA_-}{dq}\right|_{q_0}(q - q_0) + \left.\frac{d^2A_-}{dq^2}\right|_{q_0}(q - q_0)^2 + \ldots \approx \left.\frac{d^2A_-}{dq^2}\right|_{q_0} \delta q^2. \tag{41}$$

The first amplitude is a linear function of the deviation from the wave number q_0 while the second amplitude is a quadratic function of the wave number deviation.

The periodic part of the displacement field was given in the Appendix for a layer n so for the layer n=0, we have:

$$u_1(q, x) = e^{-iqx}\left(A_+ e^{ik_1 x} + A_- e^{-ik_1 x)}\right), \tag{42}$$

and expansion of this expression around q_0 gives:

$$u_1(q, x) = u_1(q_0, x) + \left.\frac{du_1}{dq}\right|_{q_0}(q - q_0) + \ldots \tag{43}$$

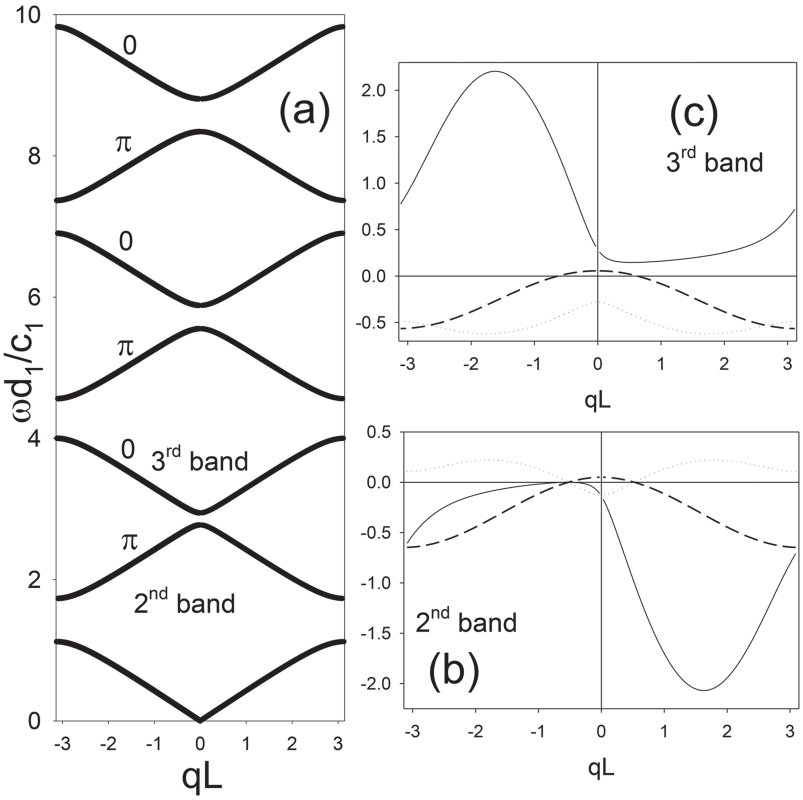

FIG. 5. (a) Band structure of one-dimensional superlattice (see text for details), real part of A_+ (dotted line), imaginary part of A_+ (dashed line) and the imaginary part of A_- (solid line) for (a) the second dispersion branch and (c) the third branch. The geometrical phase accumulated by the elastic wave as one follows a closed path in qL space is indicated on the band structure.

Inserting Eqs. (42), (40) and (41) into (43) yields:

$$u_1(q,x) \approx e^{-iq_0x} e^{ik_1^{(0)}x} \left.\frac{dA_+}{dq}\right|_{q_0} (q-q_0)\,. \tag{44}$$

The Berry connection, $BC(q)$, in wave number space, q, is calculated from the relation:

$$\frac{1}{u_1^* u_1} u_1^* \frac{du_1}{dq} = \frac{1}{(q-q_0)+i\varepsilon}. \tag{45}$$

In that expression, $u_1^* u_1$ is a normalizing factor. Equation (45) is analytically continued into the complex plane by introducing the quantity $\varepsilon \to 0$. The imaginary part of the Berry connection is the phase change, namely

$$\frac{\delta\eta}{\delta q} = \lim_{\varepsilon\to 0} \frac{-\varepsilon}{(q-q_0)^2+\varepsilon^2} = -\pi\delta(q-q_0). \tag{46}$$

This expression is valid only in the vicinity of the point (q_0, ω_0). The amplitude does not change sign elsewhere, so we anticipate that the phase change $\delta\eta = 0$ everywhere else but at q_0. Thus we extend the use of expression (46) to the entire Brillouin zone. Since there is only one point (q_0, ω_0) along the second branch in the band structure of Fig. 4, the integral of Eq. (46) over the Brillouin zone, $\eta = \int_{-\frac{\pi}{L}}^{\frac{\pi}{L}} dq \frac{\delta\eta}{\delta q}$ gives a Zak phase of $-\pi$. The third band does not possess a point (q_0, ω_0) and therefore, the Zak phase is zero. Similarly, the fourth, sixth, etc. bands exhibit a π geometrical phase while the fifth, seventh, etc. bands have a geometrical phase equal to zero.

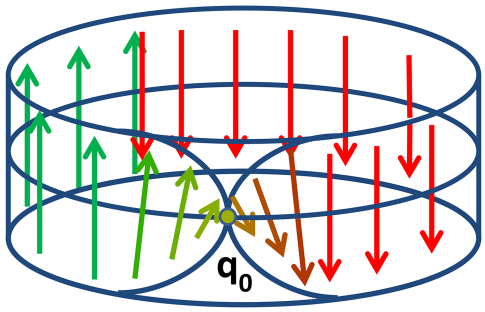

FIG. 6. Schematic illustration of a closed manifold with a single half-turn twist which topology is isomorphic to that of the eigen vectors of a superlattice along a band with a Zak phase of π.

B. Topological interpretation of the Zak phase

This topological interpretation of the geometrical phase derived for the harmonic oscillator (subsection II C) can also be applied to the Zak phase of bands in the band structure of superlattices. For instance, Eq. (46) is isomorphic to Eq. (31) where the frequency, ω, is replaced by the wave number, q. The major difference though lies in the fact that in a periodic system, such as a superlattice, the dispersion relations are periodic functions of the wave number, $q \in \left[\frac{-\pi}{L}, \frac{\pi}{L}\right]$. In this case, the topological interpretation of the Zak phase in terms of a manifold is given in Fig. 6.

The primary difference between Fig. 6 and Fig. 3 is that the manifold is formed of a closed strip in the latter case because of the periodicity in wave number, q, space. The twist may be visualized as a segment of helicoid with infinitesimally small width in q, space. The arrows in Fig. 6 illustrate parallel transport of a vector field on a closed loop on the manifold. Upon spanning the Brillouin zone once (closed path of length $\frac{2\pi}{L}$), the transported vector accumulates a phase of π. One needs to complete two turns in q space i.e., follow a closed path which length $\frac{4\pi}{L}$ to recover the original orientation of the parallel transported vector, i.e., accumulate a phase of 2π.

IV. CONCLUSIONS

We have illustrated the concept of geometric phase in the case of two prototypical elastic systems, namely the one-dimensional harmonic oscillator and a one-dimensional binary superlattice. In the first case, the well-known phase change of π of the displacement amplitude of a driven harmonic oscillator as the driving frequency crosses its characteristic frequency is interpreted topologically in terms of the parallel transport of a vector field along a curved manifold constituted of a strip containing a helicoidal twist. The twist occurs at the characteristic frequency. An elastic superlattice is known to possess dispersion bands along which the displacement amplitude changes sign and therefore exhibits a change in phase of π. In this periodic system, the geometric phase (also known as the Zak phase) is now a periodic function of the wave number. The change in phase along a path in the Brillouin zone of the superlattice is interpreted topologically in terms of the parallel transport of a vector field along a manifold constituted of a closed twisted strip. The twist occurs at the wave number where the amplitude of elastic waves changes sign. The investigation of two simple model elastic systems has the aim of illustrating the abstract concepts of geometric phase and its topological interpretation. The formal mapping of the evolution of the geometrical phase on the spectral or wave number domains onto the parallel transport of a vector field on curved manifold spanning the frequency and wave number spaces is hoped to help interpret topological features of elastic waves in more complex media such as two-dimensional or three dimensional phononic crystals and acoustic metamaterials.

ACKNOWLEDGMENTS

PAD acknowledges financial support from NSF award # 1640860.

APPENDIX: EIGEN VALUES AND EIGEN VECTORS IN ONE-DIMENSIONAL ELASTIC SUPERLATTICE

We consider a one-dimensional (1D) superlattice composed of alternating segments of material 1 and material 2. The density and speed of sound in the two types of materials are ρ_1, ρ_2 and c_1, c_2. The lengths of the alternating segments are d_1 and d_2, respectively. The 1D equation of propagation of longitudinal waves in a homogeneous medium with speed of sound c is:

$$\frac{\partial^2 u(x,t)}{\partial t^2} = c^2 \frac{\partial^2 u(x,t)}{\partial x^2}. \tag{A1}$$

We seek solutions in the form: $u(x,t) = u(x)e^{i\omega t}$. Inserting in Eq. (A1) gives:

$$-\omega^2 u(x) = c^2 \frac{\partial^2 u(x)}{\partial x^2}. \tag{A2}$$

The solution to Eq. (A2) will take the general form of quasi-standing waves:

$$u(x) = A_+ e^{ikx} + A_- e^{-ikx}, \tag{A3}$$

with $k^2 = \frac{\omega^2}{c^2}$.

We expect the solution given by Eq. (A3) to be a periodic function of position, x, with a period L. We therefore write the solution in the form of a Bloch wave, namely:

$$u(x) = e^{iqx} u(q,x), \tag{A4}$$

where the quantity $q \in \left[\frac{-\pi}{L}, \frac{\pi}{L}\right]$. The periodic function $u(q,x)$ must meet the condition $u(q,x) = u(q,x+L)$. The periodic functions in the segments 1 and 2 in the nth layer are given by:

$$u_1(q,x) = e^{-iq(x-nL)} \left(A_+ e^{ik_1(x-nL)} + A_- e^{-ik_1(x-nL)}\right), \tag{A5a}$$

$$u_2(q,x) = e^{iq(x-nL)} \left(B_+ e^{ik_2(x-nL-d_1)} + B_- e^{-ik_2(x-nL-d_2)}\right), \tag{A5b}$$

with $k_1 = \frac{\omega}{c_1}$ and $k_2 = \frac{\omega}{c_2}$. $A_\pm$ and $B_\pm$ are the amplitude of the forward and backward propagating waves in media 1 and 2, respectively.

The solutions in the segment 1 and 2 in the nth layer of the superlattice are therefore given by:

$$u_1(x) = e^{iqnL} \left(A_+ e^{ik_1(x-nL)} + A_- e^{-ik_1(x-nL)}\right), \tag{A6a}$$

$$u_2(x) = e^{iqnL} \left(B_+ e^{ik_2(x-nL-d_1)} + B_- e^{-ik_2(x-nL-d_1)}\right). \tag{A6b}$$

To find the amplitudes, we use the conditions of continuity of displacement and of stress at the interfaces.

The condition of continuity of displacement at the interface between layer n and layer n-1 (i.e. location $x = nL$ between segment 1 in layer n and segment 2 in layer n-1) states:

$$u_1(nL) = e^{iqnL}(A_+ + A_-) = u_2(nL) = e^{iq(n-1)L} \left(B_+ e^{ik_2(L-d_1)} + B_- e^{-ik_2(L-d_1)}\right),$$

which reduces to

$$A_+ + A_- = e^{-iqL} \left(B_+ e^{ik_2 d_2} + B_- e^{-ik_2 d_2}\right). \tag{A7}$$

The stress in a medium "i" is given by $\rho_i c_i^2 \frac{\partial u_i}{\partial x}$ where $\rho_i c_i^2$ is the stiffness of the medium. The continuity of stress at the interface $x = nL$ is:

$$k_1 \rho_1 c_1^2 (A_+ - A_-) = e^{-iqL} k_2 \rho_2 c_2^2 \left(B_+ e^{ik_2 d_2} - B_- e^{-ik_2 d_2}\right). \tag{A8}$$

Considering now the conditions of continuity of displacement and stress at the interface between media 1 and 2 in the same layer n, i.e., location $x = nL + d_1$ leads to:

$$A_+ e^{ik_1 d_1} + A_- e^{-ik_1 d_1} = B_+ + B_-, \tag{A9}$$

$$k_1 \rho_1 c_1^2 \left(A_+ e^{ik_1 d_1} - A_- e^{-ik_1 d_1}\right) = k_2 \rho_2 c_2^2 (B_+ - B_-), \tag{A10}$$

Equations (A7), (A8), (A9) and (A10) form a system of four linear equations in the amplitudes:

$$\begin{cases} A_+e^{ik_1d_1} + A_-e^{-ik_1d_1} - B_+ - B_- = 0 \\ A_+Fe^{ik_1d_1} - A_-Fe^{-ik_1d_1} - B_+ + B_- = 0 \\ A_+ + A_- - B_+e^{-iqL}e^{ik_2d_2} - B_-e^{-iqL}e^{-ik_2d_2} = 0 \\ A_+F - A_-F - B_+e^{-iqL}e^{ik_2d_2} + B_-e^{-iqL}e^{-ik_2d_2} = 0 \end{cases} \tag{A11}$$

where F is defined as $F = \frac{k_1\rho_1c_1^2}{k_1\rho_1c_1^2}$. This system has nontrivial solutions if the determinant of matrix: $\begin{pmatrix} \alpha_1 & \beta_1 & -1 & -1 \\ F\alpha_1 & -F\beta_1 & -1 & +1 \\ +1 & +1 & -e^{-iqL}\alpha_2 & -e^{-iqL}\beta_2 \\ F & -F & -e^{-iqL}\alpha_2 & +e^{-iqL}\beta_2 \end{pmatrix}$ is equal to zero. This condition gives the eigen values of the system. In that matrix we have introduced: $\alpha_i = e^{ik_id_i} = \frac{1}{\beta_i}$. After a number of algebraic manipulations, the eigen values are obtained from the dispersion relation:

$$\cos qL = \cos k_1d_1 \cos k_2d_2 - \frac{1}{2}\left(F + \frac{1}{F}\right)\sin k_1d_1 \sin k_2d_2. \tag{A12}$$

To solve for the Eigen values, we use the approach of transfer matrices. For this, Eqs. (A7) and (A8) can be recast in the form:

$$\begin{pmatrix} 1 & 1 \\ F & -F \end{pmatrix}\begin{pmatrix} A_+ \\ A_- \end{pmatrix}_{n+1} = e^{-iqL}\begin{pmatrix} \alpha_2 & \beta_2 \\ \alpha_2 & -\beta_2 \end{pmatrix}\begin{pmatrix} B_+ \\ B_- \end{pmatrix}_n$$

where the indices n+1 and n indicate that the amplitudes are in layers n+1 and n. The preceding equation can be rewritten as:

$$\begin{pmatrix} A_+ \\ A_- \end{pmatrix}_{n+1} = \frac{1}{2F}e^{-iqL}\begin{pmatrix} (F+1)\alpha_2 & (F-1)\beta_2 \\ (F-1)\alpha_2 & (F+1)\beta_2 \end{pmatrix}\begin{pmatrix} B_+ \\ B_- \end{pmatrix}_n. \tag{A13}$$

Equations (A9) and (A10) can be reformulated as:

$$\begin{pmatrix} 1 & 1 \\ 1 & -1 \end{pmatrix}\begin{pmatrix} B_+ \\ B_- \end{pmatrix}_n = \begin{pmatrix} \alpha_1 & \beta_1 \\ F\alpha_1 & -F\beta_1 \end{pmatrix}\begin{pmatrix} A_+ \\ A_- \end{pmatrix}_n$$

and recast in the form:

$$\begin{pmatrix} B_+ \\ B_- \end{pmatrix}_n = \frac{1}{2}\begin{pmatrix} (1+F)\alpha_1 & (1-F)\beta_1 \\ (1-F)\alpha_1 & (1+F)\beta_1 \end{pmatrix}\begin{pmatrix} A_+ \\ A_- \end{pmatrix}_n. \tag{A14}$$

In equation (A14), both sets of amplitudes are located within a layer n.

Finally, we can insert Eq. (A14) into Eq. (A13) to obtain:

$$\begin{pmatrix} A_+ \\ A_- \end{pmatrix}_{n+1} = \begin{pmatrix} t_{11} & t_{12} \\ t_{21} & t_{22} \end{pmatrix}\begin{pmatrix} A_+ \\ A_- \end{pmatrix}_n. \tag{A15}$$

The 2x2 matrix in Eq. (A15) is the transfer matrix that relates the amplitudes between two adjacent layers. The components of the transfer matrix are given by:

$$t_{11} = \frac{1}{4F}\alpha_1\left[(F+1)^2\alpha_2 - (F-1)^2\beta_2\right], \tag{A16a}$$

$$t_{22} = -\frac{1}{4F}\beta_1\left[(F-1)^2\alpha_2 - (F+1)^2\beta_2\right], \tag{A16b}$$

$$t_{12} = -\frac{1}{4F}\beta_1(F+1)(F-1)(\alpha_2 - \beta_2), \tag{A16c}$$

$$t_{21} = \frac{1}{4F}\alpha_1(F+1)(F-1)(\alpha_2 - \beta_2). \tag{A16d}$$

Note that because the modes in the periodic superlattice are Bloch modes, we can write:

$$\begin{pmatrix} A_+ \\ A_- \end{pmatrix}_{n+1} = e^{iqL}\begin{pmatrix} A_+ \\ A_- \end{pmatrix}_n.$$

With this condition, Eq. (A15) can be recast in the form of an eigen value problem:

$$\left(\begin{pmatrix} t_{11} & t_{12} \\ t_{21} & t_{22} \end{pmatrix} - e^{iqL}\begin{pmatrix} 1 & 0 \\ 0 & 1 \end{pmatrix}\right)\begin{pmatrix} A_+ \\ A_- \end{pmatrix}_n = 0. \tag{A17}$$

If e^{iqL} is an eigen value, the determinant of the matrix in the left hand side of Eq. (A17) vanishes and the system of Eq. (A17) reduces to a single equation:

$$\left(t_{11} - e^{iqL}\right) A_+ = -t_{12} A_-$$

which gives the non-normalized eigen vectors:

$$A_+ = -t_{12}, \tag{A18a}$$

$$A_- = t_{11} - e^{iqL}, \tag{A18b}$$

where we express the components of the transfer matrix in the form:

$$t_{11} = e^{ik_1 d_1}\left[\cos k_2 d_2 + \frac{i}{2}\left(F + \frac{1}{F}\right)\sin k_2 d_2\right], \tag{A19a}$$

and

$$t_{12} = -e^{-ik_1 d_1}\left[\frac{i}{2}\left(F - \frac{1}{F}\right)\sin k_2 d_2\right]. \tag{A19b}$$

Introducing $e^{\pm ik_1 d_1} = \cos k_1 d_1 \pm i \sin k_1 d_1$ into Eqs. (A19a,b) and using the dispersion relation given by Eq. (A12), one gets the complex amplitudes:

$$A_+ = \frac{1}{2}\left(F - \frac{1}{F}\right)\sin k_1 d_1 \sin k_2 d_2 + \frac{i}{2}\left(F - \frac{1}{F}\right)\cos k_1 d_1 \sin k_2 d_2, \tag{A20a}$$

$$A_- = i\left[\sin k_1 d_1 \cos k_2 d_2 + \frac{1}{2}\left(F + \frac{1}{F}\right)\cos k_1 d_1 \sin k_2 d_2 - \sin qL\right]. \tag{A20b}$$

[1] I. Newton, *Principia—Book II, Imprimatur S. Pepys* (Reg. Soc. Praeses, London, 1686).
[2] J. W. S. Rayleigh, *The Theory of Sound* (Dover, New York), two vols., 1877–78, Vol. 1.
[3] F. Schwabel, *Advanced Quantum Mechanics*, 4th Ed. (Springer, 2008).
[4] P. A. Deymier Ed., *Acoustic Metamaterials and Phononic Crystals*, Springer Series in Solid State Sciences 173 (Springer, Heidelberg, 2013).
[5] M. Z. Hasan and C. L. Kane, "Colloquium: Topological insulators," Rev. Mod. Phys. **82**, 3045–3067 (2010).
[6] A. B. Khanikaev, S. H. Mousavi, W.-K. Tse, M. Kargarian, A. H. MacDonald, and G. Shvets, "Photonic topological insulators," Nature Materials **12**, 233–239 (2013).
[7] M. C. Rechtsman, J. M. Zeuner, Y. Plotnik, Y. Lumer, D. Podolsky, F. Dreisow, S. Nolte, M. Sergev, and A. Szameit, "Photonic Floquet topological insulators," Nature **496**, 196–200 (2013).
[8] F. D. M. Haldane and S. Raghu, "Possible realization of directional optical waveguides in photonic crystals with broken time-reversal symmetry," Phys. Rev. Lett. **100**, 013904 (2008).
[9] P. A. Deymier, K. Runge, N. Swinteck, and K. Muralidharan, "Torsional topology and fermion-like behavior of elastic waves in phononic structures," Comptes Rendus Mécanique **343**, 700–711 (2015).
[10] P. A. Deymier, K. Runge, N. Swinteck, and K. Muralidharan, "Rotational modes in a phononic crystal with fermion-like behaviour," J. Appl. Phys. **115**, 163510 (2014).
[11] E. Prodan and C. Prodan, "Topological phonon modes and their role in dynamic instability of microtubules," Phys. Rev. Lett. **103**, 248101 (2009).
[12] C. L. Kane and T. C. Lubensky, "Topological boundary modes in isostatic lattices," Nat. Phys. **10**, 39–45 (2013).
[13] S. Mousavi, A. B. Khanikaev, and Z. Wang, "Topologically protected elastic waves in phononic metamaterials," Nat. Commun. **6**, 8682 (2015).
[14] B. G. Chen, N. Upadhyaya, and V. Vitelli, "Nonlinear conduction via solitons in a topological mechanical insulator," Proc. Natl. Acad. Sci. USA **111**, 13004–13009 (2014).
[15] R. Süsstrunk and S. D. Huber, "Observation of phononic helical edge states in a mechanical topological insulator," Science **349**, 47–50 (2015).
[16] M. Xiao, G. Ma, Z. Yang, P. Sheng, Z. Q. Zhang, and C. T. Chan, "Geometric phase and band inversion in periodic acoustic systems," Nat. Phys. **11**, 240–244 (2015).
[17] J. Paulose, B. G. Chen, and V. Vitelli, "Topological modes bound to dislocations in mechanical metamaterials," Nat. Phys. **11**, 153–156 (2015).
[18] N. Berg, K. Joel, M. Koolyk, and E. Prodan, "Topological phonon modes in filamentary structures," Phys. Rev. E **83**, 021913 (2011).

[19] R. K. Pal, M. Schaeffer, and M. Ruzzene, "Helical edge states and topological phase transitions in phononic systems using bi-layered lattices," J. Appl. Phys. **119**, 084305 (2016).
[20] A. B. Khanikaev, R. Fleury, S. H. Mousavi, and A. Alù, "Topologically robust sound propagation in an angular-momentum-biased graphene-like resonator lattice," Nat. Commun. **6**, 8260 (2015).
[21] G. Salerno, T. Ozawa, H. M. Price, and I. Carusotto, "Floquet topological system based on frequency-modulated classical coupled harmonic oscillators," Phys. Rev. B **93**, 085105 (2015).
[22] J. Paulose, A. S. Meeussen, and V. Vitelli, "Selective buckling via states of self-stress in topological metamaterials," Proc. Natl. Acad. Sci. USA **112**, 7639–7644 (2015).
[23] L. M. Nash, D. Kleckner, A. Read, V. Vitelli, A. M. Turner, and W. T. M. Irvine, "Topological mechanics of gyroscopic metamaterials," Proc. Natl. Acad. Sci. USA **112**, 14495–14500 (2015).
[24] P. Wang, L. Lu, and K. Bertoldi, "Topological phononic crystals with one-way elastic edge waves," Phys. Rev. Lett. **115**, 104302 (2015).
[25] Z. Yang, F. Gao, X. Shi, X. Lin, Z. Gao, Y. Chong, and B. Zhang, "Topological acoustics," Phys. Rev. Lett. **114**, 114301 (2015).
[26] N. Swinteck, S. Matsuo, K. Rung, J. O. Vasseur, P. Lucas, and P. A. Deymier, "Bulk elastic waves with unidirectional backscattering-immune topological states in a time-dependent superlattice," J. Appl. Phys. **118**, 063103 (2015).
[27] M. V. Berry, "Quantal Phase Factors Accompanying Adiabatic Changes," Proc. of the Royal Soc. A **392**, 45–57 (1984).
[28] M. P. Hobson, G. Estathiou, and A. N. Lasenby, *General Relativity – An Introduction for Physicists* (Cambridge University Press, Cambridge, 2006).
[29] J. Zak, "Berry's phase for energy bands in solids," Phys. Rev. Lett. **62**, 2747 (1989).
[30] R. E. RCamley, B. Djafari-Rouhani, L. Dobrzynski, and A. A. Maradudin, "Transverse elastic waves in periodically layered infinite and semi-infinite media," Phys. Rev. B **27**, 7318 (1983).
[31] B. Djafari-Rouhani, L. Dobrzynski, O. Hardouin Duparc, R. E. Camley, and A. A. Maradudin, "Sagittal elastic waves in infinite and semi-infinite superlattices," Phys. Rev. B **28**, 1711 (1983).